Physica D 241 (2012) 315–325

Contents lists available at SciVerse ScienceDirect

Physica D

journal homepage: www.elsevier.com/locate/physd

Time adaptive variational integrators: A space–time geodesic approach

Sujit Nair

United Technologies Research Center, East Hartford, CT 06118, United States

ARTICLE INFO

Article history:
Received 7 February 2010
Received in revised form
9 September 2011
Accepted 10 September 2011
Available online 22 September 2011
Communicated by V. Rom-Kedar

Keywords:
Euler–Lagrange
Geodesic
Variational integrators
Symplectic

ABSTRACT

The goal of this paper is to show that the space–time geodesic approach of classical mechanics can be used to generate a time adaptive variational integration scheme. The only assumption we make is that the Lagrangian for the system is in a separable form. The geometric structure which is preserved in the integration scheme is made explicit and the algorithm is illustrated with simulation for a compact case, a non-compact case, a chaotic system which arises as a perturbation of an integrable system and the figure eight solution for a three body problem.

1. Introduction

We start by giving the basic idea in coordinate notation in this section. Let (M, g) be a n-dimensional Riemannian manifold and $L : TM \to \mathbb{R}$ be the Lagrangian for a system. Let $q^i, i \in \{1, \ldots, n\}$ denote a local coordinate chart and q^i_t denote the time derivative of a curve $q^i(t)$. Let $T(q, q_t) = \frac{1}{2} g_{ij} q^i_t q^j_t$ be the kinetic energy and $V(q)$ be the potential energy of a physical system. Recall that the standard Lagrangian system with Lagrangian given by $L = T(q, q_t) - V(q)$ has the Euler–Lagrange equations of motion given by

$$q^i_{tt} + \Gamma^i_{jk} q^j_t q^k_t = -g^{ij} \frac{\partial V}{\partial q^j} \tag{1}$$

where Γ^i_{jk} is the Christoffel symbols for the metric g_{ij}. When $V = 0$, the Lagrangian L is purely kinetic energy and the equations of motion are geodesic equations of motion. In this case, we have

$$q^i_{tt} + \Gamma^i_{jk} q^j_t q^k_t = 0 \tag{2}$$

and it can be easily verified that (2) is invariant under affine time reparametrization $t \to at + b$ where a, b are constants. Indeed, (2) is derived from the following *energy action* principle

$$\delta \int T(q, q_t) dt = 0 \tag{3}$$

which itself is affine time reparametrization independent. Under an arbitrary reparametrization $t \to t(s)$, $t'(s) \neq 0$ in (3), we get

$$\delta \int T(q, q_s) \frac{ds}{dt} ds = 0. \tag{4}$$

Therefore, we see that the energy action changes under reparametrization unless $\frac{ds}{dt} = \text{constant}$, i.e., if the reparametrization is affine. Consider also the following *length action* principle

$$\delta \int \sqrt{T(q, q_\lambda)} d\lambda = 0. \tag{5}$$

For the length action, we get that under an arbitrary reparametrization $\lambda \to \lambda(s)$, $\lambda'(s) \neq 0$

$$\delta \int \sqrt{T(q, q_s)} ds = 0. \tag{6}$$

Therefore, the length action is parametrization invariant. If the physical system is in a potential free field and its Lagrangian is the kinetic energy, one can construct its trajectory $q(s) \in M$ using the length action principle. Once this is done, one can then construct the physical time evolution $q(t) \in M$ in which t is the unique parametrization which conserves the Hamiltonian of the system, again given by the Lagrangian. We now consider again the case when V is not zero. Can we still see this as a geodesic problem? In this paper, we show that it is indeed the case and that any Lagrangian system of the form $T - V$ can be recast as a geodesic problem.

Contributions and focus: Before proceeding, let us state the main contributions of this paper and issues which we do not address here.

E-mail addresses: NairSS@utrc.utc.com, nair@cds.caltech.edu.

0167-2789/$ – see front matter © 2011 Elsevier B.V. All rights reserved.
doi:10.1016/j.physd.2011.09.006

1. Our presentation here is for a general Hamiltonian system in the spirit of [1]. We show that one can indeed construct a genuine time adaptive integrator scheme and at the same time demonstrate the sense in which this time adaptive scheme is geometric. We achieve this without any assumptions like integrability, scale invariance or reversibility as in [2–4]. And neither do we want to restrict ourselves to the Kepler problem or its variations as in [5].
2. The idea of considering an extended (or higher dimensional space) space to achieve some kind of adaptivity is not new. But to the best of our knowledge, this has only been demonstrated for Kepler type problems using a combination of *Sundman transformation* and Levi-Civita or Kustaanheimo–Stiefel (LC/KS) regularization. After the extension, the resulting higher dimensional Hamiltonian is no longer regular in the momenta variable, i.e., the Hessian is not regular [5]. Moreover, this method relies crucially on the fact that the kinetic and potential parts of the extended Hamiltonian are both exactly solvable. In our approach, we do consider an extended phase space but in our case, the resulting extended Hamiltonian is a purely geodesic problem with no potential part and is regular in the extended momenta variables.

Having stated the main contributions, we would like to point out that we do not optimize the choice of time step in this paper and leave it for future work. It is an old and well known observation [6,7] that structure preserving alone does not guarantee accuracy of solutions. And for systems with complex and chaotic dynamics, one should rather look at statistical properties of solutions rather than focus on accuracy of individual solutions. We do not address these issues in this paper. Geometric structure preserving is a necessary, though not sufficient, step toward controlling accuracy of solutions and we show in this paper that one can use adaptive time stepping and still preserve some underlying geometric structure. The problem of optimizing the time steps in a systematic manner for arbitrary multidimensional Hamiltonian without any integrability, scale invariance or separability assumptions system is a highly nontrivial task. Time adaptive schemes have been very successful for scale invariant systems with or without self-similar solutions as can one fruitfully combine the scaling invariance and the Hamiltonian structure and come up with a guided approach for time stepping choice [5,8]. For example, in the Kepler problem with coordinates (q, p), the scale invariance is used to generate the heuristic $\frac{dt}{d\tau} = q^\gamma$ for the evolution of the fictive time. Once one has this heuristic, an optimization is done over the parameter γ [5]. Though time step optimization is an important issue on its own right, we do not attempt to address it here and leave it for future work. We do however illustrate our technique for a chaotic system as well has a three body problem system with a 12 dimensional phase space. See Section 5 for the relevant plots.

The outline of the paper is as follows. In Section 2 we start with a motivating example in Section 2.1 namely the Kepler problem. We show how the Newtonian approximation can be seen as a geodesic problem in space–time. Using this as a motivation, we state Proposition 1 in Section 2.2. We then discuss application of the space–time geodesic formulation to variational integrators in Section 3. Finally, we conclude with some simulation results in Section 5.

2. From Lagrangian to geodesic

In this section, we will demonstrate how to convert a standard Euler–Lagrange problem to a geodesic when the Lagrangian $L : TM \to \mathbb{R}$ is of the form $L = T - V$ where T is the kinetic energy and V is the potential energy. Before we do this, let us first consider a motivating example.

2.1. The Kepler problem

Consider the Kepler problem, both in the Newtonian case and the general relativity case [9]. Let m be the mass of the orbiting test body, M the mass of the spherically symmetric gravitating body and G the gravitational constant. The Lagrangian for the Newtonian case in polar coordinates is given by

$$L_N = \frac{1}{2}\left(\dot{r}^2 + r^2\dot{\varphi}^2\right) - V(r) \tag{7}$$

where $V(r) = -\frac{GMm}{r} + \frac{L^2}{2mr^2}$. The Euler–Lagrange equations for this Lagrangian are

$$\frac{d}{dt}(\dot{r}) = r\dot{\varphi}^2 - \frac{\partial}{\partial r}V(r)$$
$$\frac{d}{dt}\left(r^2\dot{\varphi}\right) = 0. \tag{8}$$

Now consider the general relativity version of the Kepler problem. In this case, we have a space–time metric called the Schwarzschild metric and the Lagrangian given by [9]

$$L_{GR} = \frac{1}{2}\left(\left(1 - \frac{r_s}{r}\right)c^2 t'^2 - \frac{r'^2}{\left(1 - \frac{r_s}{r}\right)} - r^2\varphi'^2\right). \tag{9}$$

Here, primes denote derivatives with respect to the proper time parameter τ and $r_s = \frac{2GM}{c^2}$ is the Schwarzschild constant which goes to zero as speed of light goes to infinity. The Euler–Lagrange equations corresponding to L_{GR} have two conserved quantities corresponding to its symmetry in t and φ variables. Note that this is a geodesic problem with the Newtonian approximation "hiding" in the form of space–time coupling. The Lagrangian also treats space and time equally in the sense that Hessian of the Lagrangian is regular (though with different signs and hence not hyperregular) in time and space variables. If one writes down the equations of motion corresponding to the Lagrangian L_{GR} in (9), it can be shown to be equivalent to those of

$$\tilde{L}_N = \frac{1}{2}\left(\dot{r}^2 + r^2\dot{\varphi}^2\right) - \tilde{V}(r) \tag{10}$$

where $\tilde{V}(r) = -\frac{GMm}{r} + \frac{L^2}{2mr^2} - \frac{GML^2}{c^2mr^3}$. One recovers the Newtonian Kepler problem in the limit $c \to \infty$. Fig. 1 illustrates the geodesic unfolding process for the Kepler problem.

2.2. The general case

The result from Section 2.1 has an analogous extension to an arbitrary Lagrangian system. Moreover, one can achieve this without changing the underlying physics of the problem. Consider the Lagrangian

$$L = \frac{1}{2}\dot{x}^2 - V(\mathbf{x}) \tag{11}$$

where $x \in \mathbb{R}$ with EL equations and initial conditions

$$\ddot{x} = -\frac{\partial V}{\partial x}; \qquad x_0 = x(0), \dot{x}_0 = \dot{x}(0). \tag{12}$$

What we now want to do is to construct a Lagrangian $\tilde{L} = \tilde{L}(x, t, x', t')$ in space–time where the primes denote derivatives with respect to some parameter λ such that (12) is embedded in the Euler–Lagrange equations of $\tilde{L}$. We have the following result from [10].

Proposition 1. *Let $x(t)$ solve (12) for some time interval $t \in [0 \;\; T]$. Consider the Lagrangian*

$$\tilde{L} = \frac{1}{2}x'^2 + \frac{1}{2V}t'^2 \tag{13}$$

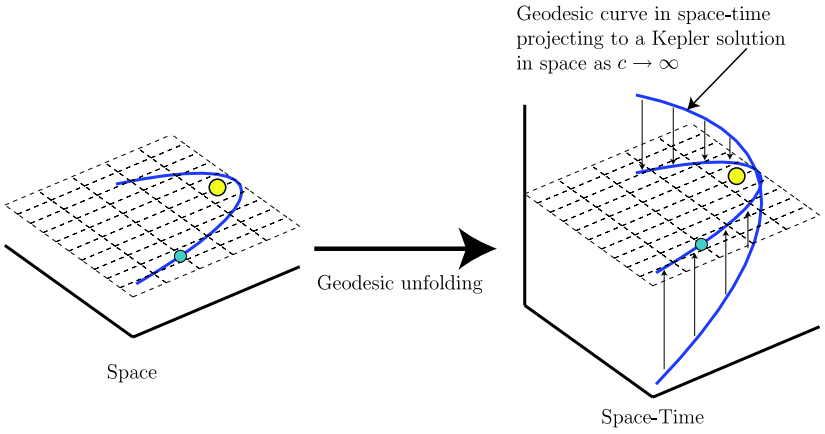

Fig. 1. Illustration of the geodesic unfolding process for the Kepler problem.

with Euler–Lagrange equations and initial conditions

$$x'' = -\frac{1}{2}\frac{1}{V^2}\frac{\partial V}{\partial x}t'^2; \quad x_0 = x(0), x_0' = \dot{x}_0 t_0' \tag{14a}$$

$$t'' = \frac{1}{V}\frac{\partial V}{\partial x}t'x'; \quad t(0) = 0, t'(0) = \alpha V(x_0). \tag{14b}$$

If $\tilde{x}(\lambda), t(\lambda)$ *solves (14) for some time interval* $\lambda \in \left[0 \ \tilde{T}\right]$*, then* $\tilde{x}(\lambda) = x(t/\beta)$ *for as long as both sides are defined. Here,* β *is a constant given by* $\frac{\sqrt{\alpha}}{2}$*. Therefore, the solutions for* x *and* $\tilde{x}$ *differ only by a constant rescaling of time.*

Proof. Since $\tilde{L}$ is independent of t, the corresponding momentum is conserved. Let $\frac{t'}{V} = \alpha$. Substituting this into (14a), we get the following system and its initial condition

$$x'' = -\frac{\alpha^2}{2}\frac{\partial V}{\partial x}; \quad x_0 = x(0), x_0' = \dot{x}_0 t_0' \tag{15}$$

(15) is a constant time rescaled version of (12) with rescaling given by $\beta = \frac{\sqrt{\alpha}}{2}$. □

Therefore, (12) transforms to a geodesic problem which can be solved using the length action or the energy action with the former lending itself to arbitrary parametrization in time. We have also achieved general covariance in the sense that one can consider an arbitrary diffeomorphism $f(x, t) = (y, s)$ of space–time which was not available when one considered the Lagrangian (11). One also sees that the Lagrangian is completely regular in the space–time variables and treats t and x equally. So the action principle in space–time we now have is

$$\delta \int_{\lambda_0}^{\lambda_1} \tilde{L}(t, \mathbf{x}, t', \mathbf{x}')d\lambda = 0 \tag{16}$$

for some arbitrary parameter λ.

Remark 1. After the initial version of this paper, it was brought to our attention by one of the reviewers that a form of Proposition 1 appears in a 1929 paper of Eisenhart [10]. The format and the title of the paper were changed to reflect this rediscovery.

Remark 2. Note that even though $\tilde{L}$ depends upon V and couples the space and time variable in a nontrivial manner, the embedded evolution equations for x only depends upon $\frac{\partial V}{\partial x}$. So one could add any constant to V without changing the x-dynamics. If the potential V is bounded or if the x-domain is compact, then one can add a large constant to make the kinetic metric $\tilde{L}$ have $(+\ +)$ or $(+\ -)$ sign globally.

Remark 3 (*Configuration Dependent Kinetic Energy*)**.** The treatment in the previous section extends directly to the case when we have kinetic energy metric depending upon the configuration variables. We did not include it to avoid unnecessary distraction. When the original system has Lagrangian $L = \frac{1}{2}g_{ij}\dot{q}^i\dot{q}^j - V(q)$, then the corresponding $\tilde{L}$ is given by $\tilde{L} = \frac{1}{2}g_{ij}q'^i q'^j + \frac{1}{2V(q)}t'^2$ and Proposition 1 holds true for this case.

Remark 4. The discrete version of Proposition 1 holds true. See (51) in Section 5.1.2.

3. Applications to numerical integration

We now apply Proposition 1 to develop time adaptive (as opposed to just being time varying) variational based numerical integration schemes for Lagrangian systems. Please see [1,11–19] for a background on variational integrators for mechanical systems and continuum mechanics. Time adaptivity is an important and crucial ingredient to reduce computational cost and in dealing with velocity regimes in different scales. This topic has been dealt with in the past using various approaches. As in [1,20] we do stress the space time approach. The main difference being that in addition to the spacetime view point, we also stress the geodesic viewpoint. Consider the scenario when we start with q_0, q_1 and the intermediate time step h_0. As noted in [1], in the time step varying case, one needs to solve for both the next position q_2 as well as h_1 using an implicit set of equations. These equations are the discrete Euler–Lagrange equations and the conservation of energy equation. In other words, we only have time varying step sizes as opposed to having a time adaptive step size where in we can use time steps at our own discretion. Moreover, this technique also fails at turning points where velocities are nearly zero. This phenomena can be traced to the Jacobi–Maupertuis principle on constant energy surface given by $\delta \int \sqrt{E - V(q)}ds = 0$ where ds corresponds to the kinetic energy metric. This principle becomes singular at turning points where the kinetic energy is zero. Our geodesic based approach in this paper is both time adaptive and has no problems near turning points. Another recent approach is using the Hamilton–Pontryagin variational principle where time reparametrization is incorporated into the variational principle and one discretizes the following action [21,22]

$$S_{HP} = \int_{\tau_1}^{\tau_2} \left[\left(\frac{1}{2}v^2 - V(q)\right)N - E(\dot{t} - N) + p(\dot{q} - vN)\right]d\tau.$$

One drawback in our opinion even with this formulation is that it still treats space and time differently. For example, the Hessian of

the Lagrangian is still singular in the time direction, i.e., linear in $\dot{t}$ but quadratic in velocity.

Before we go into the variational discretization, let us explore some properties of the continuous equations of motion, both for the length minimization and energy minimization problem. For simplicity, let us consider the following two Lagrangians

$$L_1 = \sqrt{x'^2 + f(x)t'^2} \qquad L_2 = \frac{1}{2}\left(x'^2 + f(x)t'^2\right) \tag{17}$$

where primes denote differentiation w.r.t some parameter λ. As mentioned before, the action corresponding to L_1 is invariant under arbitrary reparametrization $\lambda = \lambda(\mu), \frac{d\lambda}{d\mu} \neq 0$ whereas the L_2 action is only affine reparametrization invariant. Therefore, the Euler–Lagrange equations corresponding to L_2 are affine time reparametrization invariant. The Euler–Lagrange equations corresponding to L_1 are

$$\frac{d}{d\lambda}\left(\frac{x'}{\sqrt{x'^2 + f(x)t'^2}}\right) = \frac{\frac{\partial f}{\partial x}t'^2}{2\sqrt{x'^2 + f(x)t'^2}} \tag{18a}$$

$$\frac{d}{d\lambda}\left(\frac{f(x)t'}{\sqrt{x'^2 + f(x)t'^2}}\right) = 0. \tag{18b}$$

It is instructive to verify the reparametrization invariance in (18). If the equations in (18) are reparametrization invariant, what it means is that a solution to the two equations in (18) only gives a curve in the (x, t) space (for example $F(x, t) = 0$) and does not tell you where in the curve you will be at any time instant (for example, does not tell you $F(x(\lambda), t(\lambda)) = 0$ for some time parameter λ). For example, consider the plane $\mathbb{R}^2$ with (x, y) coordinates and the standard Euclidean metric $|\dot{\gamma}(t)| = \sqrt{\dot{x}^2 + \dot{y}^2}$. In this case, as is well known geodesics are straight lines. Consider two different parametrizations $\gamma_1(t) = (t, t)$ and $\gamma_2(t) = (t^3, t^3)$ for the straight line $y = x$. It can be verified that γ_1 and γ_2 both satisfy the Euler–Lagrange equations for the length action given by $\delta \int |\dot{\gamma}(t)| dt = 0$. Whereas, the energy action given by $\delta \int |\dot{\gamma}(t)|^2 dt = 0$ fixes the parametrization for the straight line $y = x$. $\gamma_1(t)$ is the unique parametrization which satisfies the energy action, i.e., if we have a particle in a potential free field with Lagrangian given by its kinetic energy, its time evolution is given by $\gamma_1(t)$.

Observe also that the equations in (18) seemingly look like two evolution equations which should in general tell you not only the shape of the curve but also the parametrization of the curve. How does one reconcile these two notions? The solution lies in realizing that the above two equations are in fact just one equation. After simplifying, (18a) and (18b) modifies to

$$x'\left(f\left(t'x'' - x't''\right) - \frac{1}{2}\frac{\partial f}{\partial x}t'(2x'^2 + ft'^2)\right) = 0 \tag{19a}$$

$$t'\left(f\left(t'x'' - x't''\right) - \frac{1}{2}\frac{\partial f}{\partial x}t'(2x'^2 + ft'^2)\right) = 0. \tag{19b}$$

Assuming that $x'(\lambda)$ and $t'(\lambda)$ are both not identically zero in an interval, we see that equations in (19) reduce to essentially just one equation given by

$$f\left(t'x'' - x't''\right) - \frac{1}{2}\frac{\partial f}{\partial x}t'(2x'^2 + ft'^2) = 0. \tag{20}$$

In other words, the Euler–Lagrange equations corresponding to the length action are not independent. (20) can further be reduced to the form

$$F\left(x, \frac{dx}{dt}, \frac{d^2x}{dt^2}\right) = 0 \quad \text{or} \quad F\left(t, \frac{dt}{dx}, \frac{d^2t}{dx^2}\right) = 0 \tag{21}$$

depending upon the region in the $x-t$ plane where x is a graph over t (locally) or where t is a graph over x (locally) thereby eliminating the parameter λ.

3.1. Notation

Before proceeding, let us fix some notations for the rest of the paper for clarity. The superscript p will denote the physical quantities and the superscript st will denote space–time quantities. Therefore, we have

$$L^p = \frac{1}{2}\dot{x}^2 - V(x)$$

$$L^{st} = \frac{1}{2}x'^2 + \frac{1}{2V}t'^2.$$

The physical time is denoted by τ and t denotes the "time" part of the space–time coordinates. L_d^p and L_d^{st} denote the discrete counterpart of L^p and L^{st} respectively. The exact discretization procedure will be clear from the context. The parameter stepping in physical time will be denoted by h_i and the parameter stepping in space–time setting will be denoted by λ_i. Therefore, (x_0, x_1, h_0) will denote configurations x_0, x_1 separated by physical time step h_0. And $(x_0, t_0, x_1, t_1, \lambda_0)$ will denote space–time configurations $(x_0, t_0), (x_1, t_1)$ separated by parameter λ_0. Differentiation with respect to the physical time is denoted by dot and differentiation with respect to the space–time parameter is denoted by prime. And finally, $L(q, \dot{q})$ denotes an arbitrary Lagrangian for configuration space Q with local coordinates $q \in Q$.

3.2. Variational discretization

We now list the variational discrete analogue of (20), (18a) and (18b). The main idea behind variational discretization is that one starts with the variational principle and discretizes the variational principle instead of discretizing the continuous evolution equations derived from the variational principle. We refer the reader to [16] for more details. Given a continuous Lagrangian $L(q, \dot{q})$ where q is the configuration state, the variational discrete equations are constructed as follows. If $S = \int_{t_0}^{t_1} L(q(t), q_t(t))dt$ is the continuous action, the discrete action S_d corresponding to discrete time steps $\{t_i, i = 0, \ldots, N\}$ is

$$\begin{aligned} S_d &= \sum_{i=0}^{N-1} \int_{t_i}^{t_{i+1}} L(q(t), q_t(t))dt \\ &\approx \sum_{i=0}^{N-1} h_i L\left(\frac{q_i + q_{i+1}}{2}, \frac{q_{i+1} - q_i}{h_i}\right) \end{aligned}$$

for the mid point approximation scheme. Here, $h_i = t_{i+1} - t_i$. Let

$$L_d(q_i, q_{i+1}, h_i) = L\left(\frac{q_i + q_{i+1}}{2}, \frac{q_{i+1} - q_i}{h_i}\right). \tag{22}$$

Then, the discrete action is

$$S_d = \sum_{i=0}^{N-1} h_i L_d(q_i, q_{i+1}, h_i). \tag{23}$$

The discrete variational equations are derived using the discrete action principle $\delta S_d = 0$ and are given by

$$h_i D_2 L_d(q_i, q_{i+1}, h_i) + h_{i+1} D_1 L_d(q_{i+1}, q_{i+2}, h_{i+1}) = 0 \tag{24}$$

for $i = 1, \ldots, N-1$. Computing these discrete equations for the length action given by L_1 in (17), we get that the discrete analogues of (18a) and (18b) are

$$\begin{aligned} &\frac{2(x_1 - x_0) + \frac{1}{2}\frac{\partial f}{\partial x}\big|_{\left(\frac{x_1+x_0}{2}\right)}(t_1 - t_0)^2}{d_{01}} \\ &\quad - \frac{2(x_2 - x_1) - \frac{1}{2}\frac{\partial f}{\partial x}\big|_{\left(\frac{x_2+x_1}{2}\right)}(t_2 - t_1)^2}{d_{12}} = 0 \end{aligned} \tag{25a}$$

$$\frac{f(\frac{x_1+x_0}{2})(t_1 - t_0)}{d_{01}} - \frac{f(\frac{x_2+x_1}{2})(t_2 - t_1)}{d_{12}} = 0 \tag{25b}$$

where $d_{ij} = \sqrt{(x_i - x_j)^2 + f(\frac{x_i+x_j}{2})(t_i - t_j)^2}$. Note how the equations in (25) do not have any step sizes in them. Just as in the continuous case, the equations in (25) are not independent. One can derive the discrete analogue of (20) as

$$\frac{2(x_1 - x_0) + \frac{1}{2}\frac{\partial f}{\partial x}|_{\left(\frac{x_1+x_0}{2}\right)}(t_1 - t_0)^2}{f(\frac{x_1+x_0}{2})(t_1 - t_0)} - \frac{2(x_2 - x_1) - \frac{1}{2}\frac{\partial f}{\partial x}|_{\left(\frac{x_2+x_1}{2}\right)}(t_2 - t_1)^2}{f\left(\frac{x_2+x_1}{2}\right)(t_2 - t_1)} = 0. \tag{26}$$

To solve (26) numerically, one can now choose *arbitrary* step sizes in either t or x direction and solve for the x or t respectively.

3.3. Space–time symplectic conservation

In this section, we will discuss the sense in which the variational discretization discussed in Section 3.2 is symplectic structure preserving. We first discuss the continuous case. As is well known from [19], constant time stepping algorithms cannot be symplectic, energy and momentum preserving simultaneously. In the constant time stepping case, the integration algorithm is given by a single mapping associated to the corresponding time step. If one is willing to broaden the sense in which an algorithm is symplectic, then one can make sense of the notion of symplecticity in varying or adaptive time stepping case. In this section, we give details on how our approach is symplectic in the context of adaptive time stepping case. The underlying idea is simple. We first integrate the space–time geodesic problem given by (13) which admits adaptive time stepping. Once this is done, we get a sequence of points $(x_0, t_0), \ldots, (x_n, t_n)$ in which t_i are not in general the physical time parameter. We now use the fact that the physical time and the energy given by Hamiltonian are conjugate variables to reconstruct the physical time. See section Section 3.4 below for more details on physical time reconstruction and energy conservation. The mechanical system given by the Lagrangian (13) intrinsically lives in a space–time manifold $Q \times \mathbb{R}$.

3.3.0.1. The continuous case

For the Lagrangian given by (13) the canonical symplectic structure which is preserved in the continuous case is given by

$$\Omega = dx \wedge dp_x + dt \wedge dp_t \tag{27}$$

where Ω is the canonical symplectic form on $T^*(Q \times \mathbb{R})$. Here,

$$p_x = x' \tag{28}$$

$$p_t = \frac{1}{V}t' \tag{29}$$

where the primes denote derivatives with respect to the new parameter λ which we recall is *not* the physical time.

3.3.0.2. The constant space–time stepping discrete case

We have two different cases in the discrete setting. We first discuss the constant space–time stepping technique. Recall from [16] that in this setting, the discrete algorithm is a single map $\Phi : Q \times Q \to Q \times Q$ which maps $(q_{k-1}, q_k) \mapsto (q_k, q_{k+1})$ by the discrete Euler–Lagrange (DEL) equations. The discrete fiber derivative $FL_d : Q \times Q \to T^*Q$ is also given by a single map which maps $(q_0, q_1) \mapsto (q_0, D_1L_d(q_0, q_1))$. The 2-form ω_d on $Q \times Q$ given by the pull back of the canonical two-form on T^*Q is given in coordinates by

$$\omega_d = \frac{\partial^2 L_d}{\partial q_k^i \partial q_{k+1}^j} dq_k^i \wedge dq_{k+1}^j. \tag{30}$$

Using a straightforward calculation (see [16]), one can check that the map Φ exactly preserves the symplectic form ω_d.

For the Lagrangian given by (13) with the corresponding constant space–time stepping discrete Euler–Lagrange equations, the symplectic form given by (30) is exactly preserved. In our case, the Lagrangian we are interested is given by L^{st} and the conserved discrete symplectic form is given by the space–time symplectic

$$\omega_d = \frac{\partial^2 L_d^{st}}{\partial x \partial t} dx \wedge dt. \tag{31}$$

3.3.0.3. The adaptive space–time stepping discrete case

We now consider the adaptive space–time stepping case. This is a more delicate issue to handle because we no longer have a single map in the integration algorithm. Consider F_s, the flow map of the extended Hamiltonian given in canonical coordinates by

$$F_s : (q(t), p(t), t, H) \mapsto (q(t+s), p(t+s), t+s, H). \tag{32}$$

Let ω be the canonical symplectic form on T^*Q and $\Omega_H = \omega + dH \wedge dt$ be the extended symplectic form. Then, the flow map F_s preserves the extended symplectic form [20], i.e., $F_s^*\Omega_H = \Omega_H$. In coordinates, we have

$$F_s^*\omega + dH \wedge ds = \omega. \tag{33}$$

In the adaptive stepping case, it is the discrete version of (33) which holds true. Let Φ denote the mapping which maps (q_0, q_1, λ_0) to (q_1, q_2, λ_1) under the discrete Euler–Lagrange equations. Recall that the action sum in this case is

$$S = \lambda_0 L_d(q_0, q_1, \lambda_0) + \lambda_1 L_d(q_1, q_2, \lambda_1).$$

Then, using the fact that the discrete Euler–Lagrange equation given by

$$\lambda_0 D_2 L_d(q_0, q_1, \lambda_0) + \lambda_1 D_1 L_d(q_1, q_2, \lambda_1) = 0$$

holds true, one has

$$\begin{aligned} dS &= \lambda_0 D_1 L_d(q_0, q_1, \lambda_0) dq_0 + \lambda_0 D_2 L_d(q_0, q_1, \lambda_0) dq_1 \\ &\quad + \lambda_1 D_1 L_d(q_1, q_2, \lambda_1) dq_1 + \lambda_1 D_2 L_d(q_1, q_2, \lambda_1) dq_2 \\ &\quad - E_d(q_0, q_1, \lambda_0) d\lambda_0 - E_d(q_1, q_2, \lambda_1) d\lambda_1 \\ &= \lambda_0 D_1 L_d(q_0, q_1, \lambda_0) dq_0 + \lambda_1 D_2 L_d(q_1, q_2, \lambda_1) dq_2 \\ &\quad - E_d(q_0, q_1, \lambda_0) d\lambda_0 - E_d(q_1, q_2, \lambda_1) d\lambda_1 \\ &= \Theta_L^- + \Phi^* \Theta_L^+ \end{aligned} \tag{34}$$

where

$$\begin{aligned} E_d(q_0, q_1, \lambda_0) &= -D_{\lambda_0}[\lambda_0 L_d(q_0, q_1, \lambda_0)] \\ \Theta_L^-(q_0, q_1, \lambda_0) &= \lambda_0 D_1 L_d(q_0, q_1, \lambda_0) dq_0 - E_d(q_0, q_1, \lambda_0) d\lambda_0 \\ \Theta_L^+(q_0, q_1, \lambda_0) &= \lambda_0 D_2 L_d(q_0, q_1, \lambda_0) dq_0 - E_d(q_0, q_1, \lambda_0) d\lambda_0. \end{aligned}$$

Here, Θ_L^- and Θ_L^+ are the left and right discrete versions of the one form given by $pdq - Hdt$ [16] and E_d is the discrete energy. From the definition of E_d, we have

$$\Theta_L^-(q_0, q_1, \lambda_0) + \Theta_L^+(q_0, q_1, \lambda_0) = d[\lambda_0 L_d] - E_d d\lambda_0.$$

Therefore,

$$dS = d[\lambda_0 L_d] - \theta_d^+ + \Phi^* \Theta_L^+ \tag{35}$$

where θ_d^+ is the discrete analogue of the canonical one form pdq on T^*Q and given by

$$\theta_d^+ = \Theta_L^+ + E_d d\lambda_0 = \lambda_0 D_2 L_d(q_0, q_1, \lambda_0) dq_1.$$

Taking the differential of (35) and using $d^2 = 0$ and the fact that pull back commutes with differential gives

$$\Phi^* \Omega_d = \omega_d \tag{36}$$

where $\Omega_d = -d\Theta_L^+$ is the discrete analogue of the extended symplectic form and where $\omega_d = -d\theta_d^+$ is the discrete analogue of phase space symplectic form on T^*Q. Thus the identity (36) is the discrete analogue of the identity (33) and this is the sense in which adaptive stepping is symplectic.

For the Lagrangian given by (13), since there is no potential part, the Hamiltonian is just the Lagrangian. The extended symplectic form which is preserved is given by

$$\Omega_L^{st} = dx \wedge dp_x + dt \wedge dp_t + dL^{st} \wedge d\lambda. \tag{37}$$

3.3.0.4. Comparison of our work with [1]

The symplectic form which is conserved in our approach is different from the space–time symplectic form considered in [1]. For the scheme in [1], the space–time symplectic form which is conserved is given by

$$\Omega_H = dx \wedge dp_x + dH \wedge dt. \tag{38}$$

In the same paper [1], the authors construct a *time varying* scheme (as opposed to time adaptive) which is both symplectic and energy conserving. To be consistent with the obstruction in [19], one cannot hope to conserve the canonical symplectic form and energy with constant time stepping. For the time varying scheme in [1], the discrete version of the space–time symplectic form given by (38) is shown to be conserved. This is different from our version of space–time symplectic form given by (30). That said, in the physical time reconstruction step, we show that the corresponding symplectic structure which is preserved is exactly the same as in [1]. We will provide more details in the following section.

3.4. Energy conservation and time reconstruction

In this section, we discuss the sense in which energy is conserved. This is in general a nontrivial issue in the discrete case. Consider the continuous case first. If $q(t)$ is a curve satisfying the Euler–Lagrange equations for the Lagrangian given by $L = \frac{1}{2}\dot{q}^2 - V(q)$, then the corresponding Hamiltonian $H = \frac{1}{2}\dot{q}^2 + V(q)$ is conserved along $q(t)$. Moreover, the converse is also true. If $q(t)$ is a nontrivial curve such that $H(q(t), \dot{q}(t))$ is constant, then $q(t)$ satisfies the corresponding Euler–Lagrange equations. This is no longer true in the discrete world, i.e., if $q_0, q_1, \ldots, q_n$ satisfies the discrete Euler–Lagrange equations, it is not true that the corresponding discrete energy is conserved. What one can hope for is that the discrete energy be approximately preserved. In simulations, one typically sees an oscillatory behavior for the discrete energy. In this section, we show how to reconstruct the physical time using our adaptive space–time stepping approach. Once we have solved the geodesic problem given by variational discretization of (13), we get a sequence of points $(x_0, t_0), \ldots, (x_n, t_n)$ where we recall again that $t_0, \ldots, t_n$ is not necessarily the physical time. Using this sequence of points, we use the fact that energy given by the Hamiltonian and the physical time are conjugate variables to reconstruct the physical time as follows. The discrete physical Hamiltonian (or the energy) for a system with discrete Lagrangian $L_d^p(x_0, x_1, h_0)$ is given by

$$E_d^p(x_0, x_1, h_0) = -h_0 D_3 L_d^p(x_0, x_1, h_0) - L_d^p(q_0, q_1, h_0) \tag{39}$$

where h_0 is the physical time step. Given x_0, x_1 and x_2, we solve for h_0, h_1 by solving the following two equations, one being the discrete Euler–Lagrange equations for the physical Lagrangian and the other being the corresponding physical energy conservation equation.

$$h_0 D_2 L_d^p(x_0, x_1, h_0) + h_1 D_1 L_d^p(x_1, x_2, h_1) = 0$$
$$E_d^p(x_0, x_1, h_0) - E_d^p(x_1, x_2, h_1) = 0.$$

These equations have the general form

$$f(x_0, x_1, x_2, h_0, h_1) = 0$$
$$g(x_0, x_1, x_2, h_0, h_1) = 0 \tag{40}$$

where h_0, h_1 are the unknown variables. The equations in (40) are in general nonlinear equations and one requires good nonlinear solvers to tackle them numerically. The way we choose to solve (40) is by minimizing the quantity

$$\mathcal{B}(x_0, x_1, x_2; h_0, h_1) = [f(x_0, x_1, x_2, h_0, h_1)]^2 + [g(x_0, x_1, x_2, h_0, h_1)]^2. \tag{41}$$

Therefore, we have

$$(h_0, h_1) = \arg \min_{(\tilde{h}_0, \tilde{h}_1)} \mathcal{B}(x_0, x_1, x_2; h_0, h_1) \tag{42}$$

with the constraint $h_0, h_1 > 0$.

3.4.0.5. Symplectic structure preservation for physical time reconstruction

As mentioned earlier in Section 3.3, when we integrate the space–time Lagrangian to generate $(x_0, t_0), \ldots, (x_n, t_n)$, the symplectic structure that is preserved is given by (31) for constant space–time stepping and is given by (37) for adaptive space–time stepping. When we reconstruct the physical time by solving (40), the symplectic structure which is preserved is the same as the physical space–time symplectic structure given by the discrete analogue of (38).

3.4.0.6. Comparison of our work with [1]

In [1] where the authors develop time varying symplectic, energy conserving scheme, at each iteration the known variables are x_0, x_1, h_0 and one needs to solve for x_2, h_1. The equations which need to be solved are given by (40) and the same optimization technique is adopted. Therefore, in [1], the authors solve the following problem

$$(x_2, h_1) = \arg \min_{(\tilde{x}_2, \tilde{h}_1)} \mathcal{B}(x_0, x_1, x_2; h_0, h_1) \tag{43}$$

with the constraint $h_1 > 0$. The main difference being, in our case, we have already solved for the state variables x_0, x_1, x_2 using space–time geodesic approach where we essentially "forget" the physical time, which we reconstruct using the fact that it is the variable conjugate to the energy Hamiltonian. And since we are unfolding the dynamics to a higher dimensional space, we also do not face the turning point problem which the authors in [1] face because in our case, the energy in space–time never becomes zero.

Remark 5. Note that the set of equations given by (40) are in general highly nonlinear. We implicitly assume that these equations are well posed and have positive solutions. Studying regularity issues of (40) is beyond the scope of this work.

4. Summary of the main algorithm

Before proceeding to the simulation section, we summarize our algorithm. The basic steps are

1. Solve the discrete space–time Euler–Lagrange equations to get space–time coordinates $(x_0, t_0), \ldots, (x_n, t_n)$
   In this step, the symplectic structure which is preserved is given by (31) for constant space–time stepping and is given by (37) for adaptive space–time stepping.
2. Reconstruct the physical time by solving (40)
   In this step, the symplectic structure which is preserved is the discrete analogue of (38) and by construction, the discrete energy is preserved as well.

To conclude, the approach we take to numerically solve (40) is by the minimizing procedure in (42). Our algorithm is symplectic in the sense spelled out in Section 3.3 and by design it is energy conserving.

5. Simulation

We now present simulation results for the main ideas in this paper. We consider two examples, a simple pendulum with compact configuration space given by the one dimensional torus T^1 and a double well potential system with a non-compact configuration space $\mathbb{R}$ with unbounded potential.

5.1. The simple pendulum

Consider the simple pendulum with Lagrangian given by $L = \frac{1}{2}\dot{\theta}^2 - V(\theta)$ where the potential energy $V(\theta) = -\cos(\theta)$. The equations of motion are

$$\dot{\theta} = \omega \tag{44a}$$

$$\dot{\omega} = -\sin(\theta). \tag{44b}$$

5.1.1. Continuous case

The continuous space–time Lagrangians we consider are

$$L_1 = \sqrt{\theta'^2 + \frac{t'^2}{V}} \tag{45}$$

$$L_2 = \frac{1}{2}\theta'^2 + \frac{1}{2}\frac{t'^2}{V}. \tag{46}$$

Here L_1 corresponds to the length action case and L_2 corresponds to the energy action case.

5.1.1.1. Energy action. We first consider the energy case. The equations of motion corresponding to L_2 are

$$\theta'' = -\frac{1}{2}\frac{1}{V^2}\frac{\partial V}{\partial \theta}t'^2 \tag{47a}$$

$$t'' = \frac{1}{V}\frac{\partial V}{\partial \theta}t'\theta'. \tag{47b}$$

For our simulation, we choose the following initial conditions $\theta(0) = \pi/4, \theta'(0) = 0, t(0) = 0, t'(0) = \sqrt{2}V(\theta(0))$. Such an initial condition ensures that the pendulum dynamics is embedded in the L_2 Lagrangian dynamics without any time rescaling.

5.1.1.2. Length action. The equation of motion for L_1 is

$$f\left(t'\theta'' - \theta' t''\right) - \frac{1}{2}\frac{\partial f}{\partial \theta}t'(2\theta'^2 + f t'^2) \tag{48}$$

where $f = -\frac{1}{\cos(\theta)}$. As stated earlier, we can choose *any* parametrization for t. For our simulation, we choose

$$t' = \frac{1}{1.1}\left(0.1 + \frac{\theta^2}{\theta(0)}\right). \tag{49}$$

Such a parametrization ensures that when the velocity is high, i.e., when the pendulum is at its lowest point near $\theta = 0$, the time sampling gets larger. In particular, when θ is at its maximum value of $\theta(0)$ and velocity is small, $t' = 1$ and when θ is at its minimum value of 0 and velocity is large, $t' = 0.091$. Once we plug in this choice of t' and solve (48) and get $\theta(\lambda)$ as a solution, we need to reconstruct time parameter for the geodesic using $t(\lambda) = \frac{0.1}{1.1}\lambda + \frac{1}{1.1\theta(0)}\int \theta^2(\lambda)d\lambda$. To get the physical time from $t(\lambda)$, one needs another reconstruction step using the fact that L_2 is conserved for the physical system. Please see Fig. 2 for simulation plots illustrating these results.

5.1.2. Discrete adaptive time variational integrator

We start with the discrete Lagrangian given by

$$L_{2d}(\theta_0, \theta_1, h_0) = \frac{1}{2h_0}\left((\theta_1 - \theta_0)^2 + \frac{(t_1 - t_0)^2}{V\left(\frac{\theta_1+\theta_0}{2}\right)}\right) \tag{50}$$

and the corresponding discrete Euler–Lagrange equations

$$2\frac{\theta_1 - \theta_0}{h_0} - \frac{(t_1 - t_0)^2 V'(\bar{\theta}_{01})}{2V(\bar{\theta}_{01})^2 h_0} - 2\frac{\theta_2 - \theta_1}{h_1} - \frac{(t_2 - t_1)^2 V'(\bar{\theta}_{12})}{2V(\bar{\theta}_{12})^2 h_1} = 0 \tag{51a}$$

$$\frac{t_1 - t_0}{h_0 V(\bar{\theta}_{01})} - \frac{t_2 - t_1}{h_1 V(\bar{\theta}_{12})} = 0. \tag{51b}$$

Here, $\bar{\theta}_{ij}$ is the mean of θ_i and θ_j. Equations in (51) demonstrate that Proposition 1 holds true even in the discrete case. For our simulation, instead of solving (51), we will instead solve (26) with $f(\theta) = -\frac{1}{\cos(\theta)}$. For adaptivity, we choose the following step sizing

$$t_{i+1} - t_i = \begin{cases} 0.05 & \text{if } |\theta_i| \le 0.2, \\ 0.2 & \text{if } |\theta_i| > 0.6. \\ 0.1 & \text{otherwise} \end{cases} \tag{52}$$

After the numerical integration, we get a sequence of points $(\theta_0, t_0), (\theta_t, t_1), \ldots, (\theta_n, t_n)$ where the t_is are not necessarily the physical time. Using the procedure outlined in Section 3.4, we reconstruct the physical time for the system. Fig. 3 illustrates a simulation done with adaptive time stepping given by (52).

5.2. Double well potential

Now consider the double well potential system considered in [1]. The Lagrangian for this system is given by

$$L = \frac{1}{2}\dot{x}^2 - V(x) \tag{53}$$

where $x \in \mathbb{R}$ and $V(x) = \frac{1}{2}\left(x^4 - x^2\right)$. The discrete Lagrangian is given by

$$L_d(x_0, x_1, h_0) = \frac{1}{2}\left(\frac{x_1 - x_0}{h_0}\right)^2 - V(\frac{x_1 + x_0}{2})$$

with the corresponding discrete energy

$$E_d(x_0, x_1, h_0) = \frac{1}{2}\left(\frac{x_1 - x_0}{h_0}\right)^2 + V\left(\frac{x_1 + x_0}{2}\right).$$

The initial condition for our simulation is $x_0 = x_1 = 0.74$. For the constant time stepping case, we choose $h = 0.1$. For the space–time adaptive stepping case, we (arbitrarily) choose

$$\lambda_i = \begin{cases} 0.01 & \text{if } |x - 0.67| < 0.1 \\ 0.01 & \text{if } |x - 0.74| < 0.1 \\ 0.001 & \text{otherwise.} \end{cases} \tag{54}$$

Note that the λ_is are the stepping sizes for the discrete space–time Lagrangian corresponding to (53). Once we have solved for $(x_0, t_0), \ldots, (x_n, t_n)$, we reconstruct the physical time as outlined in Section 3.4. The results are plotted in Fig. 4. In the top figure, we plot the computed position x_i versus the physical time. The black squares denote the positions generated using the constant time stepping variational integrator with physical time step $h = 0.1$. The red circles denote the position data generated with the space–time adaptive steps given by (54) and with physical time reconstruction outlined in Section 3.4. As one can see, the variation in energy for the space–time adaptive scheme is negligible in comparison to the energy oscillations for the constant time stepping method. One can try to further optimize the choice of adaptive steps but we do not pursue it in this paper.

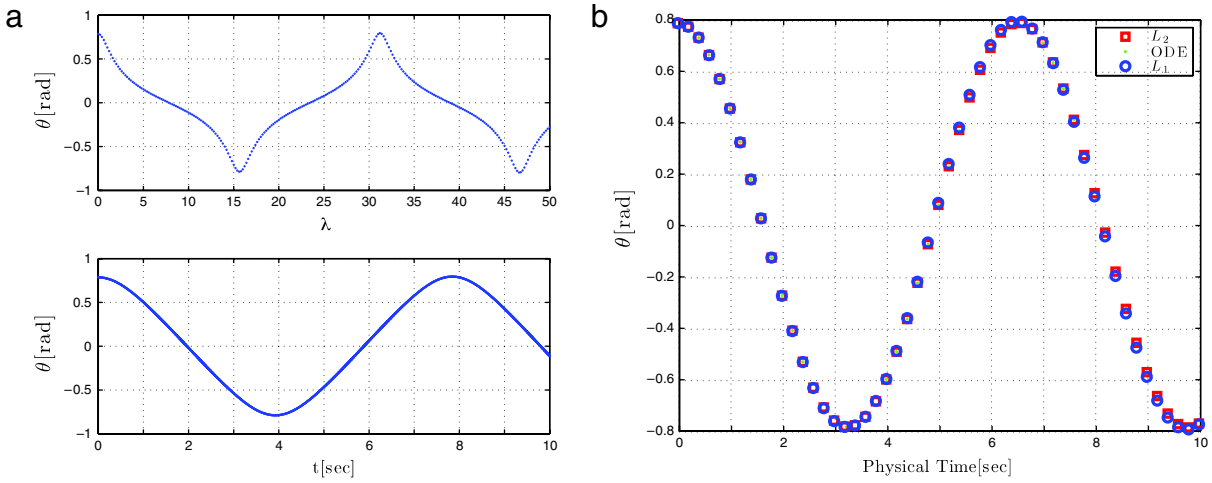

Fig. 2. (a) Plot of θ versus λ and θ versus t. Here t is the physical time which preserves L_2 and λ is an arbitrary parametrization for physical time given by (49). (b) Plot of θ versus physical time t using fourth order Runge–Kutta. The three legends in the plot correspond to (44) (ODE), (47) (L_2) and (48) (L_1) with the choice of $t'(\lambda)$ given by (49).

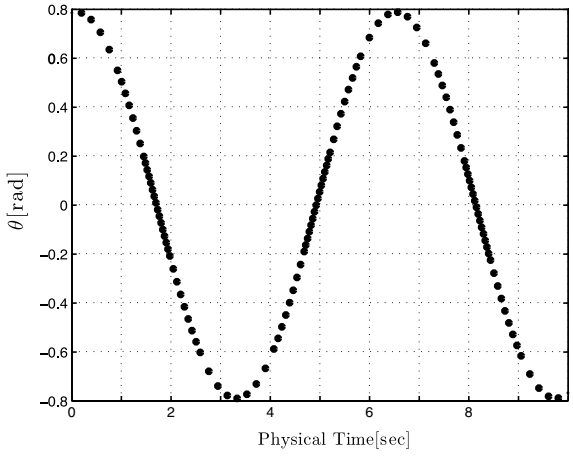

Fig. 3. Pendulum simulation using variational integrator with adaptive time stepping as specified in (52).

Remark 6. Just as in the previous examples, one can use arbitrary time stepping in the multidimensional case as follows. Since the Hamiltonian $H(q, p) = T(q, p) + V(q)$ is conserved for the physical system and we know the initial conditions, we can choose our adaptive time stepping based on the current potential $V(q)$. For example, if the initial energy is E_0, we could choose

$$t_{i+1} - t_i = \begin{cases} 0.05 & \text{if } E_0 - V(q) \geq 0.2, \\ 0.2 & \text{if } E_0 - V(q) < 0.6. \\ 0.1 & \text{otherwise} \end{cases} \tag{55}$$

and still preserve the underlying geometry as discussed in Section 4.

5.3. A chaotic system

To illustrate Remark 6 and to demonstrate that our technique can be applied to a system which is not integrable or scale invariant or which is not a variant of Kepler problem, we present simulation for a chaotic system in this section. The system we consider is obtained by coupling the double-well potential system with an oscillator system. The system has Lagrangian

$$L = \frac{1}{2}\left(\dot{x}^2 + \dot{y}^2\right) - V(x) - \frac{1}{2}y^2 + \varepsilon xy. \tag{56}$$

Here, $V(x) = \frac{1}{2}\left(x^4 - x^2\right)$ and ε is a perturbation parameter which makes the integrable double-well system a chaotic system. Fig. 5 illustrates trajectories obtained by a constant time stepping variational integrator and our adaptive time stepping integrator. The initial conditions are chosen to be $x_0 = y_0 = x_1 = y_1 = 1$ and $\varepsilon = 0.01$. For the variational integrator, the step size was chosen to be 0.1. For the adaptive scheme, the step choice was

$$\lambda_i = \begin{cases} 0.15 & \text{if } V(x) + \frac{1}{2}y^2 - \varepsilon xy > 0.1 \\ 0.1 & \text{otherwise.} \end{cases} \tag{57}$$

This ensures that the step size is small in regions where potential is small, i.e., the kinetic energy is higher. Fig. 5 presents the trajectory behavior and the energy behavior for the standard scheme and the adaptive scheme. Even though the initial conditions are the same, the trajectory drifts apart after 50 s because of the inherent chaotic nature of the system.

5.4. The figure eight (F8) solution in three body problem

We now demonstrate our method for the recently discovered F8 solution in the three body problem. The F8 solution is a special solution of the three body problem first discovered numerically [23,24] and then proven analytically [25]. As of writing this paper, it is unknown whether this solution is KAM stable but numerical evidence suggests that it is [26]. For the F8 solution, the masses of the three bodies are all chosen to be one and so is the gravitational constant. The system has a 12 dimensional phase space with the Lagrangian given by

$$\begin{aligned} &L(x_1, y_1, x_2, y_2, x_3, y_3, \dot{x}_1, \dot{y}_1, \dot{x}_2, \dot{y}_2, \dot{x}_3, \dot{y}_3) \\ &\quad = \frac{1}{2}\sum_{i=1}^{3}\left(\dot{x}_i^2 + \dot{y}_i^2\right) - V(x_1, y_1, x_2, y_2, x_3, y_3) \end{aligned} \tag{58}$$

where

$$V(x_1, y_1, x_2, y_2, x_3, y_3) = -\sum_{1\leq i<j\leq 3} \frac{1}{\sqrt{(x_i - x_j)^2 + (y_i - y_j)^2}}. \tag{59}$$

The initial conditions for the F8 solution are given by

$$(x_1, y_1) = (-0.97000436, 0.24308753) \tag{60a}$$
$$(x_2, y_2) = -(x_1, y_1) \tag{60b}$$
$$(x_3, y_3) = (0, 0) \tag{60c}$$
$$(\dot{x}_1, \dot{y}_1) = -\frac{(\dot{x}_3, \dot{y}_3)}{2} \tag{60d}$$
$$(\dot{x}_2, \dot{y}_2) = -\frac{(\dot{x}_3, \dot{y}_3)}{2} \tag{60e}$$
$$(\dot{x}_3, \dot{y}_3) = (0.93240737, 0.86473146). \tag{60f}$$

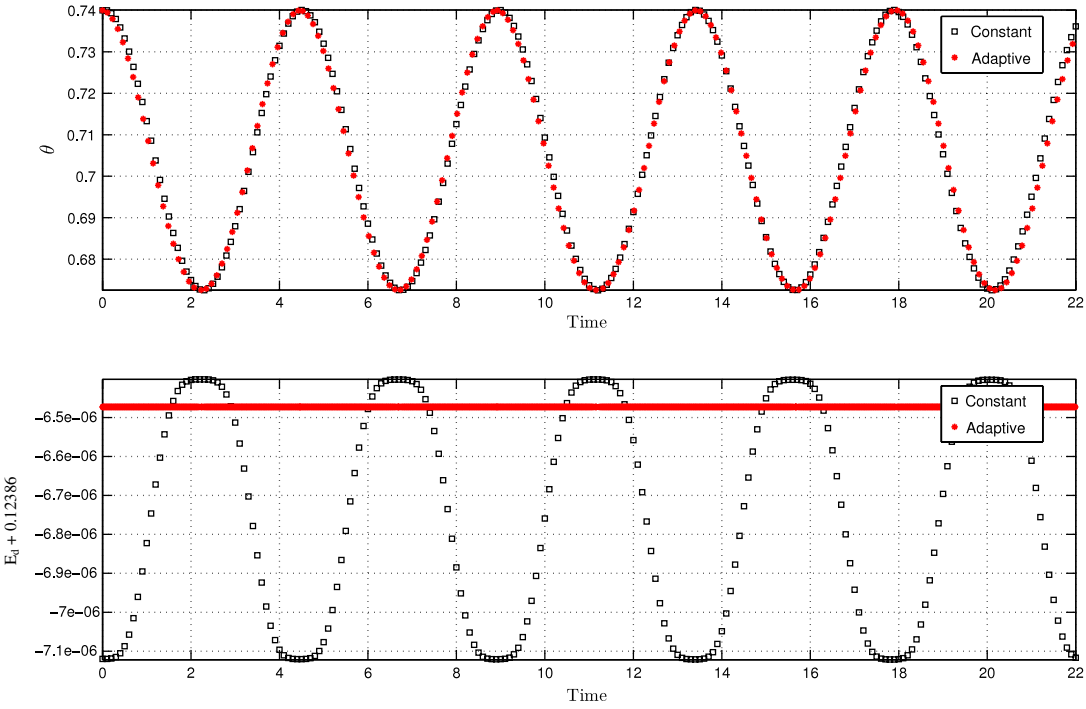

Fig. 4. Top: plot of θ versus the physical time for the double well potential. Bottom: plot of the discrete energy (shifted by 0.12386) versus the physical time for the double well potential. For both of these plots, black squares denote the data for a constant time stepping variational integrator and the red circles denote the data for the adaptive time stepping variational integrator.

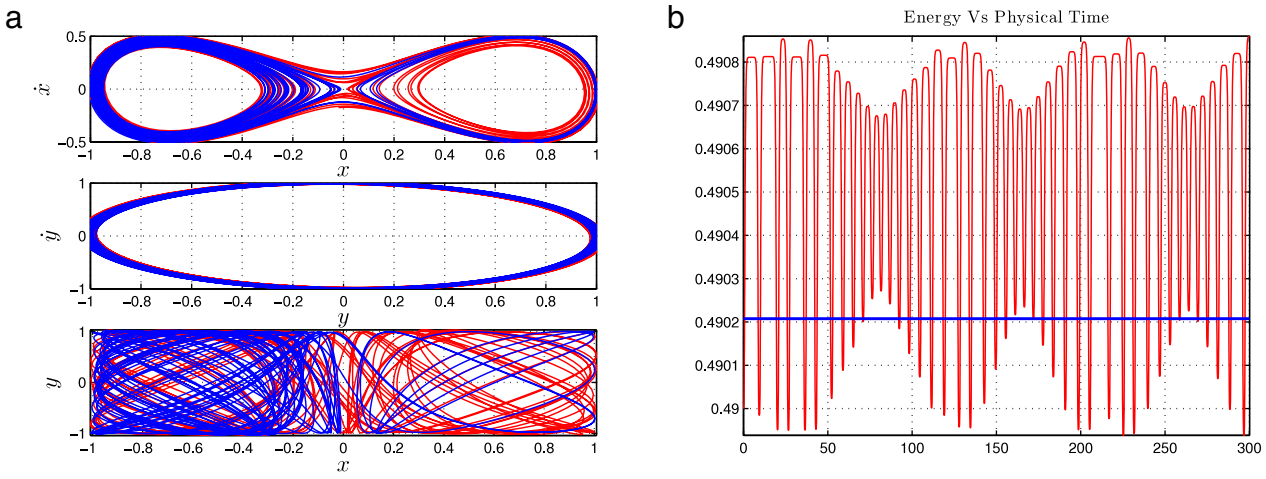

Fig. 5. (a) From top to bottom, the plots are the projection of chaotic trajectories onto $(x, \dot{x})$, $(y, \dot{y})$ and (x, y) planes respectively. The red one corresponds to constant time stepping variational integrator and blue one corresponds to adaptive time stepping variational integrator. Both of these trajectories start with the same initial condition but because of the underlying chaotic nature of the system, the trajectories drift apart after about 60 s. (b) Plot of energy versus physical time t for a constant time stepping variational integrator (red) and adaptive time stepping (blue). Note that the energy variation for the blue curve is negligible compared to the red curve.

For the adaptive stepping, we choose the stepping size to be dependent on the current potential energy. To be more precise, we choose

$$\lambda_i = \begin{cases} 0.15 & \text{if } V > -2.6 \\ 0.1 & \text{otherwise.} \end{cases} \tag{61}$$

Figs. 7 and 6 compares the standard variational integrator with step size 0.1 and 0.15 with our adaptive stepping scheme with the choice made in (61). As one can see, the energy variation is negligible compared to the variational integrator scheme and at the same time, the individual trajectory behavior is also excellent.

6. Conclusion

In this paper, we have developed and presented a framework to generate time adaptive variational and geometric integration scheme for Lagrangian systems of the form kinetic minus potential energy. The method starts by first unfolding the standard Euler–Lagrange system to its space–time manifold and recasting it as a geodesic problem without any potential energy part. The sense in which this scheme is symplectic and energy preserving is illustrated and simulation results are presented. We do not try to optimize the choice of step sizing and keep it arbitrary in this paper. Our approach here was to keep the formulation general and

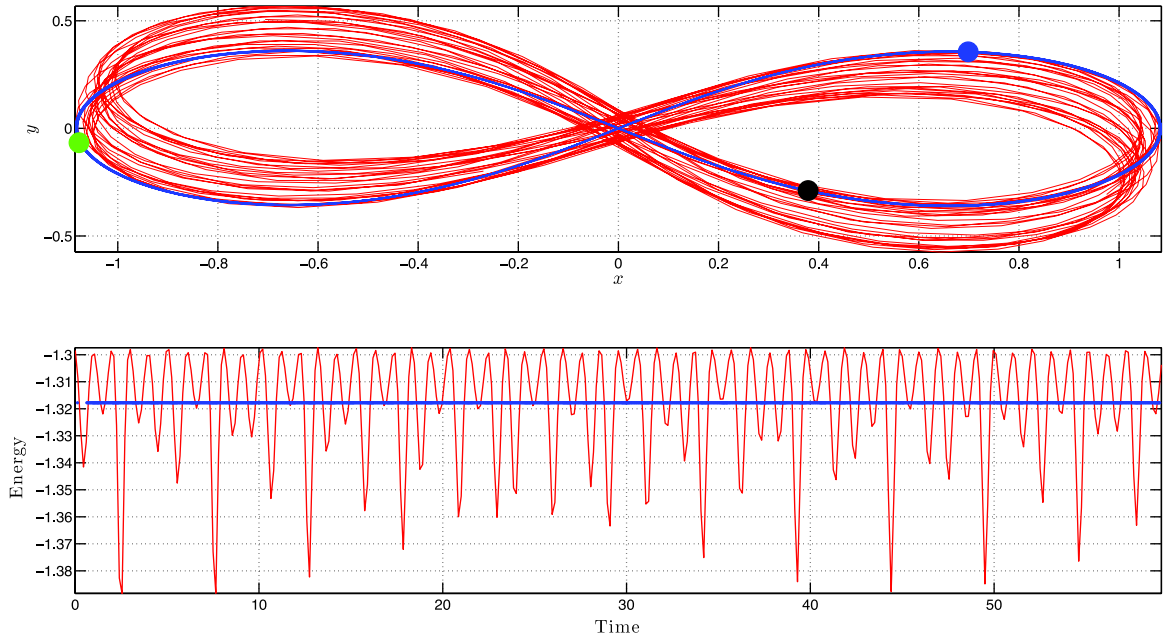

Fig. 6. Top: plot of projection of the three trajectories onto the (x, y) plane. The red curve is the trajectory for the standard variational integrator with a stepsize of 0.15 and the blue curve is the trajectory for the adaptive stepping with stepsize (61). The green, black and blue disks are the positions of the three bodies at the end of the simulation. Bottom: plot of the energy behavior for the standard variational integrator and our adaptive stepping integrator scheme. As one can see, the variation in the energy for the adaptive scheme is negligible in comparison. (For interpretation of the references to colour in this figure legend, the reader is referred to the web version of this article.)

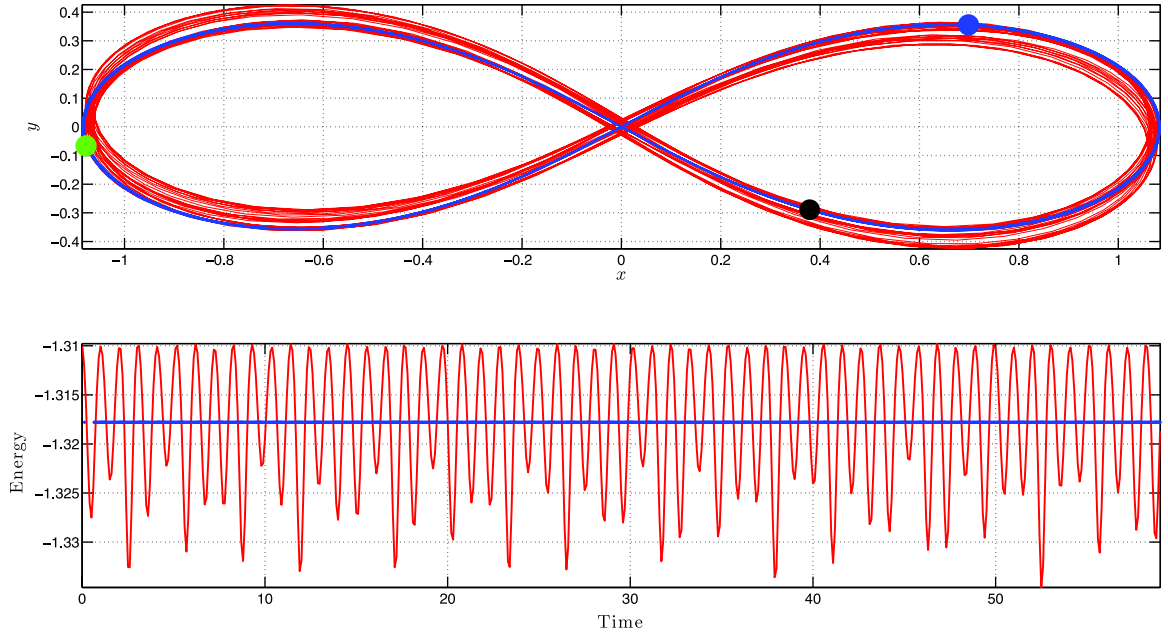

Fig. 7. Top: plot of projection of the three trajectories onto the (x, y) plane. The red curve is the trajectory for the standard variational integrator with a stepsize of 0.1 and the blue curve is the trajectory for the adaptive stepping with stepsize (61). The green, black and blue disks are the positions of the three bodies at the end of the simulation. Bottom: plot of the energy behavior for the standard variational integrator and our adaptive stepping integrator scheme. As one can see, the variation in the energy for the adaptive scheme is negligible in comparison. (For interpretation of the references to colour in this figure legend, the reader is referred to the web version of this article.)

not make any assumptions about scaling invariance, integrability or solvability. And neither did we want to restrict ourselves to Kepler type problem. We showed that one can use the space–time geodesic formulation of [10] to generate an adaptive scheme and still preserve some underlying geometric structure. Though structure preservation is not sufficient for individual trajectory error control, it is a necessary step. It is an interesting future work to use our approach and generate an optimal time stepping scheme. Ideally, one would like to construct a cost function based on a combination of "geometric error" and "individual trajectory error" which needs to be minimized over the choice of step sizes. Making this intuition precise for an arbitrary multidimensional system without any assumptions of invariance or integrability is a challenging task and remains to be done for future work. For our simulation, we choose four systems to illustrate the scheme for a compact, non-compact, chaotic and a high dimensional system.

Acknowledgments

The author would like to thank the anonymous reviewers whose comments and suggestions drastically improved the

content of this paper. We thank the anonymous reviewer for bringing to our attention the 1929 paper of L. P. Eisenhart [10] which contains a form of Proposition 1.

References

[1] C. Kane, J.E. Marsden, M. Ortiz, Symplectic energy–momentum preserving variational integrators, J. Math. Phys. 40 (7) (1999) 3353–3371. [Online]. Available: http://jmp.aip.org/resource/1/jmapaq/v40/i7/p3353_s1?isAuthorized=no.
[2] E. Hairer, Explicit, time reversible, adaptive step size control, SIAM J. Sci. Comput. 26 (6) (2005) 1838–1851.
[3] S. Blanes, C.J. Budd, Adaptive geometric integrators for hamiltonian problems with approximate scale invariance, SIAM J. Sci. Comput. 26 (4) (2005) 1089–1113.
[4] M. Preto, S. Tremaine, A class of symplectic integrators with adaptive time step for separable hamiltonian systems, The Astronomical Journal 118 (5) (1999) 2532.
[5] S. Blanes, C. Budd, Explicit adaptive symplectic (easy) integrators: a scaling invariant generalisation of the levi-civitaand ks regularisations, Celest. Mech. Dyn. Astron. 89 (2004) 383–405.
[6] J.C. Simo, O. Gonzales, Assessment of energy–momentum and symplectic schemes for stiff dynamical systems, in Proc. ASME Winter Annual Meeting, New Orleans, December 1993.
[7] M. Ortiz, A note on energy conservation and stability of nonlinear time-stepping algorithms, Comput. Struct. 24 (1) (1986) 167–168. [Online]. Available: http://www.sciencedirect.com/science/article/pii/0045794986903469.
[8] G.I. Barenblatt, Scaling, Self-similarity, and Intermediate Asymptotics, vol. 14, Cambridge University Press, Cambridge, 1996, [Online]. Available: http://www.loc.gov/catdir/description/cam027/95048212.html.
[9] C.W. Misner, K.S. Thorne, J.A. Wheeler, Gravitation, W. H. Freeman and Co., San Francisco, CA, 1973.
[10] L.P. Eisenhart, Dynamical trajectories and geodesics, Ann. of Math. 30 (1/4) (1929) 591–606.
[11] R.C. Fetecau, J.E. Marsden, M. Ortiz, M. West, Nonsmooth Lagrangian mechanics and variational collision integrators, SIAM J. Appl. Dyn. Syst. 2 (3) (2003) 381–416. electronic.
[12] C. Kane, J.E. Marsden, M. Ortiz, M. West, Variational integrators and the Newmark algorithm for conservative and dissipative mechanical systems, Internat. J. Numer. Methods Engrg. 49 (10) (2000) 1295–1325.
[13] S. Lall, M. West, Discrete variational Hamiltonian mechanics, J. Phys. A 39 (19) (2006) 5509–5519.
[14] A. Lew, J.E. Marsden, M. Ortiz, M. West, Asynchronous variational integrators, Arch. Ration. Mech. Anal. 167 (2) (2003) 85–146.
[15] A. Lew, J.E. Marsden, M. Ortiz, M. West, Variational time integrators, Internat. J. Numer. Methods Engrg. 60 (1) (2004) 153–212.
[16] J.E. Marsden, M. West, Discrete mechanics and variational integrators, Acta Numer. 10 (2001) 357–514.
[17] G. Patrick, C. Cuell, Error analysis of variational integrators of unconstrained lagrangian systems, Numerische Mathematik (2009).
[18] M. West, C. Kane, J.E. Marsden, M. Ortiz, Variational integrators, the Newmark scheme, and dissipative systems, in: International Conference on Differential Equations, Vol. 1, 2, Berlin, 1999, World Sci. Publ., River Edge, NJ, 2000, pp. 1009–1011.
[19] G. Zhong, J.E. Marsden, Lie–Poisson Hamilton–Jacobi theory and Lie–Poisson integrators, Phys. Lett. A 133 (3) (1988) 134–139.
[20] J.E. Marsden, G. Patrick, S. Shkoller, Multisymplectic geometry, variational integrators, and nonlinear pdes, Comm. Math. Phys. 199 (1998) 351–395.
[21] L. Kharevych, P. Mullen, S. Leyendecker, Y. Tong, J.E. Marsden, M. Desbrun, Robust time-adaptive integrators for computer animation (2009) (in preparation).
[22] T.M. Tyranowski, Hamilton-pontryagin variational integrators, Notes (2009).
[23] C. Moore, Braids in classical dynamics, Phys. Rev. Lett. 70 (24) (1993) 3675–3679.
[24] C. Moore, M. Nauenberg, New periodic orbits for the n-body problem, Journal of Computational and Nonlinear Dynamics 1 (4) (2006) 307–311.
[25] A. Chenciner, R. Montgomery, A remarkable periodic solution of the three-body problem in the case of equal masses, ANN.OF MATH. 2 (152) (2000) 881–901. no. 3 [Online]. Available: http://www.citebase.org/abstract?id=oai:arXiv.org:math/0011268.
[26] D. Saari, A. Chenciner, Celestial Mechanics: Dedicated to Donald Saari for his 60th Birthday: Proceedings of an International Conference on Celestial Mechanics, December 15–19, 1999, Northwestern University, Evanston, Illinois, in: Contemporary Mathematics, vol. 292, American Mathematical Society, Providence, RI, 2002.